Beamforming of Antenna for ISAC Using Antenna-on-Display

Keita Iimura*, Dongseop Lee**, Wonbin Hong**

***Dai Nippon Printing co., Ltd., Saitama, Japan**

****Pohang University of Science and Technology (POSTECH), Pohang, Republic of Korea**

Abstract

Antenna-on-display (AoD) enables mobile devices to incorporate antennas with a large footprint by integrating the topology within the display surface. Simultaneous integration of sensing and communication (ISAC) requires dual functionalities for antennas, enabling leaky wave antennas to be an effective solution for ISAC AoD. This paper provides a comprehensive analysis and demonstration of an AoD embedded within a mobile terminal, operating at millimeter-wave frequencies for both radar and wireless communication.

Author Keywords

AoD; ISAC; LWA; Transparent Antenna Film; Metal Mesh Film

1. Introduction

Integrated sensing and communication (ISAC) is increasingly being investigated for various future wireless scenarios such as 6G and non-terrestrial network (NTN) [1]. Directing a beam in a specific direction is known as beamforming. One application of ISAC is to improve communication efficiency by using radar to sense a target and focusing the direction of communication. Another potential application is incorporating radar-based gesture functions into mobile devices with existing communication capabilities. However, space in mobile devices is limited when antennas for communication and sensing are mounted separately. Therefore, it is proposed to use a single antenna element to cover both communication and sensing for ISAC [2]. As shown in Figure 1, ISAC requires antennas to meet differing needs for wireless communication and radar. A broadband antenna is necessary to cover both frequencies, and a leaky wave antenna (LWA) provides wide bandwidth but is large. Antenna-on-display (AoD) technology allows large antennas to be mounted on the display surface without taking up internal space [3]. Using a metal mesh for the electrode makes the antenna transparent and reduces resistance compared to indium tin oxide (ITO), enhancing gain. This study fabricated a prototype ISAC antenna with a metal mesh, demonstrating phase and frequency scanning beamforming with a 1 × 8 array antenna.

2. Design of metal mesh pattern

First, the transmission characteristics of metal mesh patterns were investigated. The study in [4] fabricated a patch antenna and confirmed that aligning the direction of the transmission line with the direction of the low resistance of the diamond-shaped mesh contributes to the gain improvement. In the present study, a transmission line pattern model of grounded coplanar waveguide (GCPW) was fabricated using four types of mesh structures. The structure is shown in Figure 2, where the GCPW features a solid electrode for the probed area, while a mesh is used in the other wiring areas. The unit cells of the metal mesh included diamond, hexagon, and square. Metal mesh pitches of 100 and 200 μm were utilized. Transmission line lengths of 20 mm were prepared.

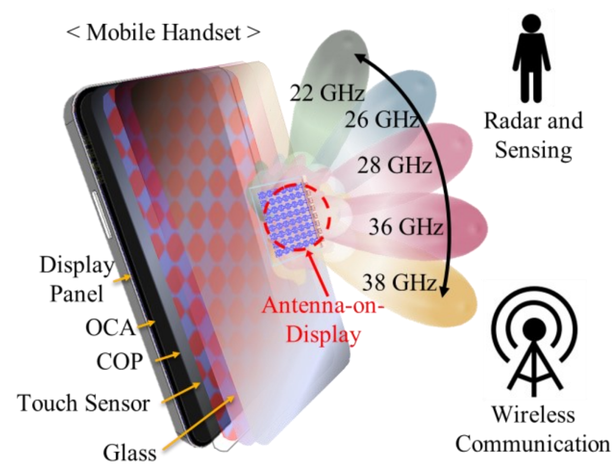

Figure 1. Concept of integrated sensing and communication (ISAC) using AoD

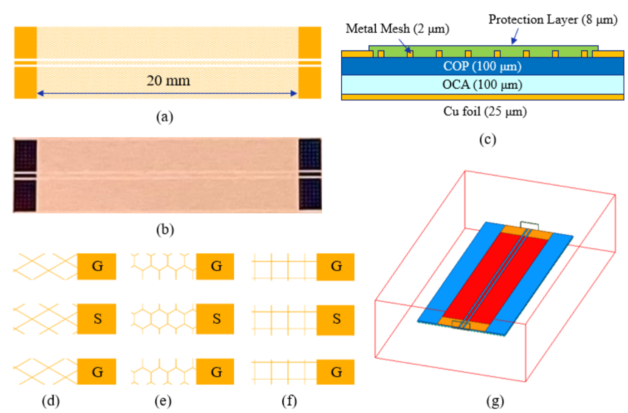

Figure 2. S_{21} evaluation pattern
(a) Transmission line design (b) Fabricated sample (c) Cross sectional view (d) Diamond mesh (e) Hexagon mesh (f) Square mesh (g)Sim. model

The transmittance and resistance values of the mesh are shown in Table 1. There is a trade-off: as the pitch of the metal mesh decreases, the resistance decreases, but transmittance also decreases. Considering the balance between transmittance and resistance, a pitch of 100 μm to 200 μm is within a practical range. Resistance can be greatly reduced when the metal mesh shape is diamond in case of the same metal density. Hexagon and square are similar, but hexagon is marginally better.

ISSN 0097-996X/25/5601-0075-$1.00 © 2025

Table 1. Resistance and transmittance of metal mesh

Mesh ID	Shape	Width (µm)	Height (µm)	Pitch (µm)	Metal Density (%)	Transmittance (%)	Resistance (Ω/sq)	Conductivity (S/m)
1	Diamond	2	2	100	4.0	87.4	0.28	1.8×10^6
2	Diamond	2	2	200	2.9	89.2	0.58	8.8×10^5
3	Hexagon	2	2	100	4.0	87.4	0.42	1.2×10^6
4	Square	2	2	100	4.0	87.4	0.43	1.2×10^6
ISAC	Diamond	2	2	120	3.3	88.0	0.34	1.5×10^6

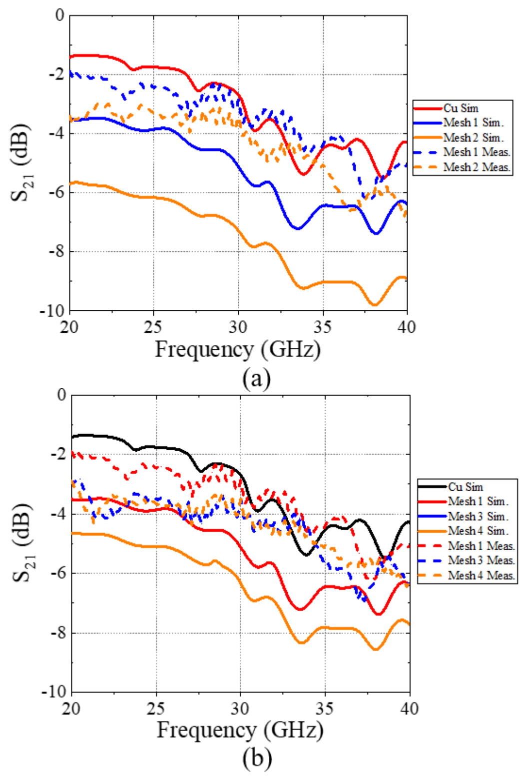

Figure 3. S_{21} measurement results
(a) Effect of mesh pitch (b) Effect of mesh shape

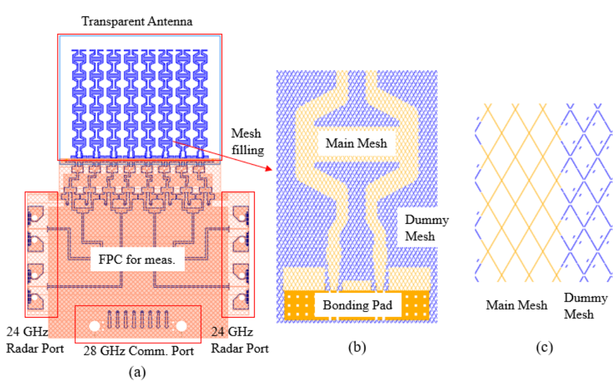

Figure 4. Design of the antenna for ISAC [5]
(a) Overview (b) Mesh filling (c) Boundary between main and dummy mesh

The results of the S_{21} measurements using these patterns are shown in Figure 3. Figure 3(a) compares mesh 1 and mesh 2 to illustrate the effect of pitch. Mesh 1 with 100 µm pitch is 0.8 dB/20 mm higher at 28 GHz than mesh 2 with 200 µm pitch. Figure 3(b) compares mesh 1, mesh 3, and mesh 4 to illustrate the effect of shape. The diamond mesh (mesh 1) is 1.4 dB/20 mm higher at 28 GHz than the hexagonal mesh (mesh 3) and the square mesh (mesh 4). The outcomes for both hexagonal and square configurations are comparable. These results confirm that diamond with a small pitch has good high-frequency transmission characteristics. The graph also shows the results of a simulation model created as shown in Figure 2(g) which was simulated using the conductivity values of the meshes shown in Table 1. The results indicated that the S_{21} of the metal mesh tended to be higher than the values estimated from the conductivity at DC. Based on these findings, diamond was selected for the shape of the next ISAC antenna prototype, and a pitch of 120 µm was chosen based on transmittance considerations.

3. Design of ISAC antenna

This section describes the antenna design for ISAC. The antenna design for ISAC utilizes LWA configuration, also known as a traveling wave antenna (TWA), to achieve gain over a wide bandwidth. The antenna design is shown in Figure 4. For more details on the ISAC antenna design, refer to [5]. The main components include a film section with a transparent antenna element, a flexible printed circuit (FPC) section for feeding, and a bonding section for connections. The film section is made of cyclo olefin polymer (COP) substrate with a dielectric constant of 2.3 and a dielectric loss tangent of 0.0005.

The bandwidth of the LWA is controlled by the structure of the unit cell, and the gain is adjusted by connecting the unit cells in series. As the number of series connections increases, the gain also increases, but saturation occurs beyond a certain point. In the lateral direction of the antenna design, a total of eight arrays were utilized for beamforming by phase shift. The LWA is particularly characterized by its capability to perform beamforming by varying the frequency [6]. By employing both phase scanning and frequency scanning beamforming, this antenna for ISAC is capable of 2-D beamforming. A diamond mesh was employed for the antenna section of the ISAC. As explained in section 2, gain can be improved by orienting the diamond in the main direction of travel (longitudinal) within the diamond mesh structure. Dummy mesh was placed around the main mesh to enhance its invisibility. The dummy mesh is cut for each unit diamond.

4. Antenna prototyping and results

The ISAC antenna was prototyped and measured. First, a transparent antenna film was fabricated. The metal mesh used for the transparent antenna was fabricated using a semi-additive process specially designed for patterning copper, achieving a line width and height of 2 µm. Figure 5 shows an enlarged view of the fabricated mesh. Figure 5(a) shows the fabricated transparent antenna film. The antenna elements are transparent and not visible, except for the bonding pads, which are visible at the bottom. Figures 5(e) and 5(f) are enlarged photographs under a microscope.

FPC is then fabricated. The FPC consists of three metal layers and the base film is polyimide (PI). The layers are Cu 9 µm / PI 25 µm / Bonding sheet 25 µm / Cu 9 µm / PI 50 µm / Cu 9 µm and plated with 15 µm on both sides for the total thickness of 160 µm. An anisotropic conductive film (ACF) crimping process was used to connect the FPC and the transparent antenna film.

This transparent antenna film with FPC is laminated on the display. Laminated in the order of cover glass 550 µm / optically clear adhesive (OCA) 200 µm / antenna film 100 µm / OCA 200 µm / panel as shown in Figure 5(d). OCA is as thick as 200 µm because it needs to be thicker than FPC. The panel functions as a ground layer. The actual prototype mimics this display configuration, using copper foil laminated in place of the panel. A photograph of the final prototype is shown in Figure 5(c). The antenna section is transparent, so the copper foil on the back side is visible, while the antenna elements themselves cannot be seen. The cable is attached to the FPC section to observe the beamforming pattern.

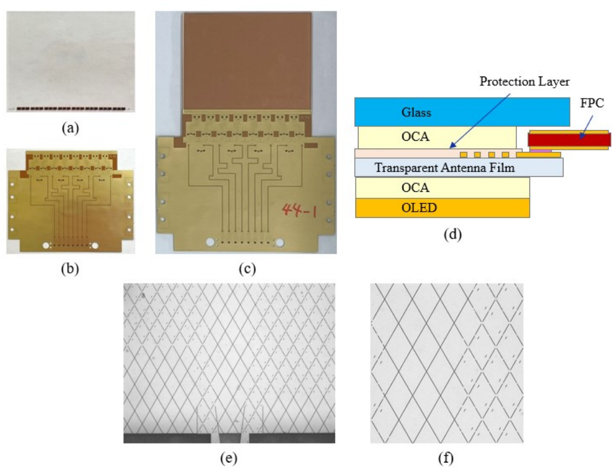

Figure 5. Photograph of prototypes
(a) Transparent antenna film (b) FPC (c) Prototype (d) Layer configuration (e) Enlarged metal mesh (f) Further enlargement

The results of the beamforming tests are presented in Figure 6. Figure 6(a) illustrates a beam scanning in the xoz plane, which is possible by varying the frequency. Scan angles ranging from -50° to + 45° were achieved using frequencies from 22 GHz to 38 GHz, with a maximum gain of 10 dBi at 28 GHz in the 0° direction. Figure 6(b) illustrates a beam scanning in the yoz plane with phase differences applied to each of the eight ports. By using a frequency of 28 GHz and a phase difference of 120°,

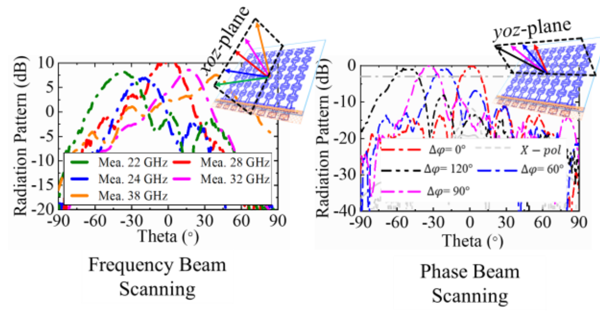

Figure 6. Beam steering pattern in antenna for ISAC [5]
(a) Frequency beam scanning (b) Phase beam scanning

a beam scan angle of up to 60° was achieved. Thus, it was confirmed that beam scans in different planes are possible depending on the frequency and phase difference, and that 2-D beamforming can be achieved by combining these two axes.

5. Conclusion

A prototype AoD using an LWA was created for the ISAC antenna. This antenna covers both radar and communication bands and enables 2-D beamforming via frequency and phase. Such antennas, designed for mobile device display, will advance the ISAC concept significantly.

6. References

1. D. Ma, N. Shlezinger, T. Huang, Y. Shavit, M. Namer, Y. Liu, and Y. C. Eldar, “Spatial Modulation for Joint Radar-Communications Systems: Design, Analysis, and Hardware Prototype,” IEEE Trans. Veh. Technol., vol. 70, no. 3, pp. 2283-2298, Mar. 2021.
2. D. Lee and W. Hong, “A Wideband Co-Linearly Polarized Sub-Grid Array Antenna-on-Display (AoD) Concept for Integration of Sensing and Communication Systems,” Proc. IEEE Int. Symp. Antennas Propag. Italy, pp. 257-258, Jul. 2024.
3. J. Park, S. Y. Lee, J. Kim, D. Park, W. Choi and W. Hong, “An Optically Invisible Antenna-on-Display Concept for Millimeter-Wave 5G Cellular Devices”, IEEE Trans. Antennas Propag., vol. 67, no. 5, pp. 2942-2952, May. 2019.
4. K. Iimura, D. Lee, W. Hong, “A Study on the Influence of Metal Mesh Design on a Transparent Antenna on Display for Radar and Communication using Ultra Fine Mesh Film,” Proc. Asia-Pacific Microw. Conf. (APMC), Indonesia, Nov. 2024.
5. D. Lee and W. Hong, “Traveling Wave Antenna-on-Display featuring Simultaneous 2-D Phase and Frequency Beam Scanning for Integrated Sensing and Communication,” Proc. European Conf. Antennas Propag., Sweden, Mar. 2025.
6. C. Caloz, T. Itoh, Electromagnetic Metamaterials: Transmission Line Theory and Microwave Applications, Hoboken, New Jersey. John Wiley & Sons, Inc., 2006.